AGU
ADVANCING EARTH AND SPACE SCIENCES

Geophysical Research Letters®

Key Points:

- Outer subsidence of tropical cyclones favors the formation of thermal circulations and ozone pollution
- Multiple thermal circulations in opposite directions cause relay transport of ozone, prolonging the duration of ozone pollution
- Urbanization alters thermal circulations via increased urban land use and anthropogenic heat, exacerbating urban ozone pollution

Relay Transport of Ozone Due To Urbanization-Modified Thermal Circulations During Tropical Cyclones

Chenchao Zhan[1,2] ![ORCID], Min Xie[3], Tijian Wang[4] ![ORCID], and Hai Guo[2] ![ORCID]

[1]School of Atmospheric Physics, Nanjing University of Information Science and Technology, Nanjing, China, [2]Department of Civil and Environmental Engineering, The Hong Kong Polytechnic University, Hung Hom, China, [3]School of Environment, Nanjing Normal University, Nanjing, China, [4]School of Atmospheric Sciences, Nanjing University, Nanjing, China

Abstract Thermal circulations are important for ozone transport and are affected by synoptic weather systems and urbanization. In this study, based on in-situ observations and numerical simulations, changes in thermal circulations induced by urbanization in Suzhou and their impacts on ozone pollution during tropical cyclone Jongdari were investigated. We found that calm weather conditions due to subsidence on the tropical cyclone periphery were conducive to the formation of sea breeze, lake breeze and ozone pollution. The sea and lake breezes had opposite directions, resulting in relay transport of ozone. When polluted air masses passed through, urban areas experienced repeated ozone pollution. Furthermore, urbanization altered the surface energy balance through increased urban land use (LU) and anthropogenic heat (AH) release, raising urban temperature and enhancing urban heat island circulation. This led to higher ozone concentrations in urban areas, especially where urban LU and AH emissions were concentrated, further exacerbating ozone pollution.

Plain Language Summary Tropical cyclones are among the most destructive weather systems, but as they approach, the subsidence on their periphery facilitates thermal circulations and ozone pollution. Multiple thermal circulations interactions may lead to relay transport of ozone, thereby prolonging the duration of ozone pollution. In addition, urban expansion due to urbanization further aggravates urban ozone pollution and increases the risk of urban population being exposed to ozone pollution. Decentralizing urban areas can be a solution to avoid this problem.

1. Introduction

Tropospheric ozone (O_3) is a secondary air pollutant produced by chemical reactions between volatile organic compounds (VOCs) and nitrogen oxides (NO_x, composed of NO and NO_2) in the presence of sunlight (Atkinson, 2000). Exposure to elevated O_3 is detrimental to public health and terrestrial vegetation (Lelieveld et al., 2015; Monks et al., 2015). In China, the implementation of the toughest-ever clean air policy, known as the Air Pollution Prevention and Action Plan from 2013 to 2017, has led to remarkable reductions in sulfur dioxide (SO_2), NO_x and particulate matter nationwide (Zhang et al., 2019; Zhao et al., 2021). However, O_3 concentrations in the megacity clusters of China have been increasing in recent years (Li et al., 2020; Liu & Wang, 2020), and O_3 pollution poses a serious challenge to China's current air quality management (Wang, Xue, et al., 2022, Wang, Parrish, et al., 2022; Wei et al., 2022). The global mean lifetime of tropospheric O_3 is about 22 days (Goldberg et al., 2015; Young et al., 2013). Long lifetime of O_3 facilitates its transport across cities and regions, making O_3 pollution control very difficult (Gong et al., 2020; Xue et al., 2014). Therefore, clarifying transport processes of O_3 has always been a primary objective in the management of O_3 pollution.

Thermal circulations with at least two reversals of wind direction in a day, such as sea-land breezes, lake-land breezes and mountain-valley breezes, have an important impact on O_3 pollution, especially for cities along the coast, near mountains, or in basins (Iannarelli et al., 2022; Sullivan et al., 2016). Once multiple thermal circulations act simultaneously, the transport of O_3 becomes extremely complex (Miao et al., 2017; Ribeiro et al., 2018). Thermal circulations are inherently driven by surface thermal contrast, and their onset, end and intensity may change because of urbanization (Li et al., 2016; You et al., 2019). As urbanization radically alters the surface water and energy balances through increasing urban land use (LU) and anthropogenic heat (AH) release (Flanner, 2009; Jiang et al., 2008). These changes have a profound influence on urban climate and in turn air quality. For example, Liao et al. (2015) found that urban expansion causes the temperature and O_3 in the Yangtze River Delta to increase by 0.9°C–2.3°C and 1.7–2.3 ppb. Ryu et al. (2013) reported that AH affects the

structure of the boundary layer, resulting in an increase in O_3 by 3.8 ppb in the Seoul metropolitan area. However, changes in thermal circulations induced by increased LU and AH due to urbanization, and the subsequent effects on O_3 transport still remain unclear.

Traditional view holds that thermal circulations and air pollution are prominent in near-calm weather conditions (Arnfield, 2003; Oke et al., 2017). However, recent studies show that air pollution is sometimes observed during severe weather conditions (Kang et al., 2019; Zhang et al., 2020). A typical example is that O_3 pollution in eastern China during summer is often associated with tropical cyclones (TCs) (Jiang et al., 2015; Wang et al., 2017). As TCs approach, the weather is usually characterized by strong radiative, high temperature and weak wind under the control of TC peripheral circulation (Deng et al., 2019; Zhan et al., 2020). Such weather conditions spark our contemplation on whether thermal circulations can form, how urbanization changes thermal circulations, and what impact these changes have on O_3 pollution during TCs. To address the above issues, this study conducts an in-depth analysis of a case of O_3 pollution caused by a landing TC in eastern China based on in-situ observations. Also, a state-of-the-art chemical transport model is employed to examine the impacts of increased LU and AH from urbanization on O_3 pollution with updated geographic data and AH emissions. These findings can fill knowledge gaps about O_3 pollution formation affected by multiple thermal circulations and be readily extended to other rapidly developing regions susceptible to TCs.

2. Study Area, Data and Methods

2.1. Suzhou

Suzhou (120.56°E, 31.41°N) is one of the most developed and densely populated cities in China, about 20 km east of Lake Taihu and 200 km west of the Yellow Sea (Figure S1 in Supporting Information S1). Due to the special geographic location, Suzhou is easily affected by lake-land breezes and sea-land breezes (Li et al., 2015; Zhang et al., 2011). Over the past 40 years, Suzhou has experienced rapid urbanization, with its population increasing from 5.2 million in 1980 to 12.8 million in 2020, and its gross domestic product (GDP) increasing from 4.1 billion to 2.2 trillion. The rapid urbanization has led to a significant increase in urban LU and AH (Tian et al., 2016). At present, the proportion of construction land in Suzhou is close to 30% (Figure S2 in Supporting Information S1), and the AH flux in the city center can reach 50 W/m^2 (Figure S3 in Supporting Information S1). Urbanization is also an important driving force for the deterioration of air quality, especially the frequent O_3 pollution in recent years (Zhan et al., 2021; Zhang et al., 2023).

2.2. Data

Air pollutants, including O_3 and its precursors (NO_2 and CO) are monitored hourly by the China National Environmental Monitoring Center (CNEMC). These data are strictly in accordance with the national monitoring standards HJ 654–2013 (http://english.mee.gov.cn/Resources/standards/Air_Environment/). The maximum daily 8 hr average (MDA8) O_3 is calculated using hourly O_3 with at least 18 hr of measurements in the day. Meteorological data, including temperature at 2 m (T_2), relative humidity at 2 m (RH), and wind speed (WS_{10}) and direction at 10 m (WD_{10}), are provided by the China Meteorological Administration (CMA) with a time resolution of 1 hr. Manual inspection, identification and handling of invalid data are performed following the methods of our previous studies (Zhan and Xie, 2022a, 2022b). Information about TCs, such as location and intensity of the TC, is obtained from the TC best track dataset issued by the CMA (Lu et al., 2021). In this study, these aforementioned data are used not only to review O_3 pollution episode but also to evaluate model performance.

2.3. The WRF-CMAQ Simulations

The one-way coupling model WRF-CMAQ, composed of the Weather Research and Forecast (WRF, version 3.9.1) model and the Community Multiscale Air Quality (CMAQ, version 5.3.2) model, is applied to simulate the O_3 pollution episode in Suzhou during TC Jongdari. In this study, WRF adopts three nested domains with horizontal resolutions of 25, 5, and 1 km and grids of 181 × 161, 186 × 181 and 201 × 196 (Figure S1 in Supporting Information S1). Vertically, there are 45 σ levels from surface to 50 hPa with 14 levels located below 2 km to resolve boundary layer processes. CMAQ uses the same vertical levels but one grid is cut from each side of WRF horizontal domains. WRF generates offline meteorological inputs for CMAQ with initial and boundary conditions from the National Centers for Environmental Prediction (NCEP) Final Analyses (FNL). The main physic parameterizations in WRF include the Thompson scheme (Thompson et al., 2008) for microphysics, the
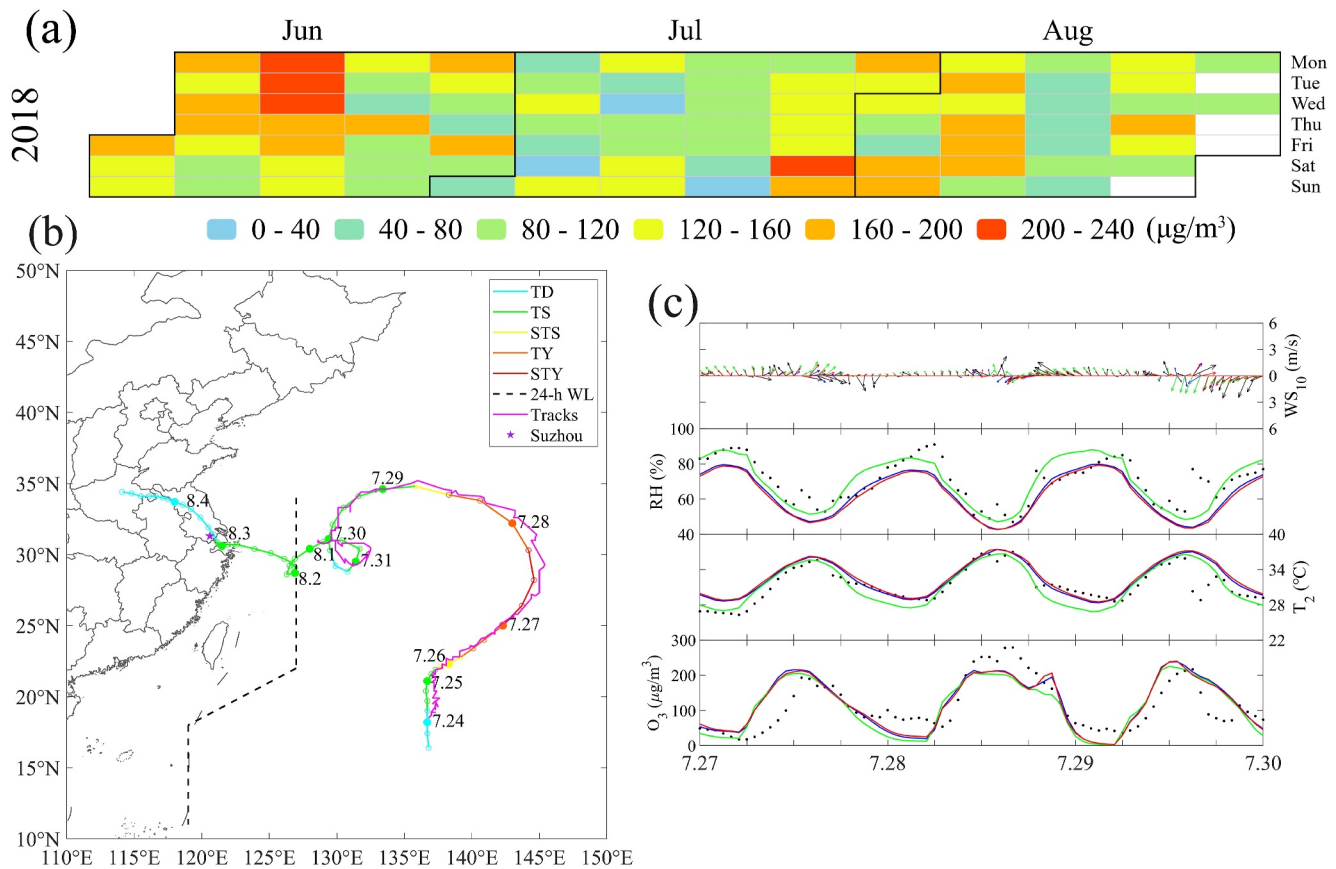
Figure 1. (a) Calendar heatmap of MDA8 O_3 concentrations in Suzhou in the summer of 2018. Blank means missing data. The Chinese national O_3 air quality standard is that MDA8 O_3 does not exceed 160 µg/m^3. (b) The observed (colored line) and simulated (magenta line) tracks of TC Jongdari with dates marked (in month.day). TD, TS, STS, TY, STY represent the intensity of TC Jongdari from weak to strong as tropical depression, tropical storm, severe tropical storm, typhoon and super typhoon (Table S2 in Supporting Information S1). The dotted back line is the 24 hr waring line for TCs. The purple five-pointed star shows the locations of Suzhou. (c) Time series of O_3, T_2, RH and WS_{10} for observations and simulations from July 27 to 30. The black dots or arrows are observations. The simulations of USGS-noAH, GLC-noAH and GLC-AH are shown in green, blue and red lines or arrows, respectively.

RRTMG scheme (Iacono et al., 2008) for longwave and shortwave radiation, the MYJ scheme (Janjic, 1994) for planetary boundary layer processes, the Kain-Fritsch Scheme (Kain, 2004) for cloud physics processes, and the Noah scheme (Tewari et al., 2004) for land surface processes. CMAQ uses the cb6r3_ae7_aq chemical mechanism. The anthropogenic emissions are provided by the Multi-resolution Emission Inventory for China (MEIC) in 2017 with a resolution of 0.25° (Zheng et al., 2018).

To examine the impacts of urbanization-induced LU and AH changes on O_3, three numerical experiments are designed, including (a) USGS-noAH, which uses USGS LU and does not add AH as baseline simulation; (b) GLC-noAH, which uses updated GLC LU and does not add AH; (c) GLC-AH, which uses updated GLC LU and adds AH. To remove uncertainties indued by model configurations, all three numerical experiments use the same domains, parameterization schemes and emissions, running from 00:00 UTC 20 July to 00:00 UTC 1 August 2018 with the first 96 hr as spin-up time. The default USGS LU in the WRF is based on the 1992–1993 1 km Advanced Very High Resolution Radiometer data, which refers to urban distribution in the late 1980s. The 30 m Resolution Global Land Cover (GLC) is based on all images acquired by Landsat-8 in 2017, which refers to the latest urban distribution (Gong et al., 2019). The AH flux is based on the statistical data of energy consumption of China in 2016. Details on the calculation of AH flux and how to add it to the WRF model can be found in Xie et al. (2016a, b). The differences between GLC-noAH and USGS-noAH thus represent the changes caused by LU, and the differences between GLC-AH and GLC-noAH represent the changes caused by AH.

To evaluate the model performance, the simulation results are compared with the observational data (Figures S3 and S4 in Supporting Information S1). As shown in Figure 1b, the simulated track of TC Jongdari almost

coincides with the observed one. Figure 1c further shows the simulated and observed time series of O_3, T_2, RH, WS_{10}. The diurnal variations of these variables are well-captured, with the correlation coefficients ranging from 0.75 to 0.78, 0.85 to 0.86, 0.80 to 0.86 and 0.40 to 0.50 for O_3, T_2, RH and WS_{10}, respectively. The magnitudes of simulation results are also acceptable, with the corresponding normalized mean biases ranging from -1.0% to 6.1%, -0.4%–3.8%, -0.8% to -11.8% and -8.8% to -28.6%, respectively (See Table S1 in Supporting Information S1 for more detailed information). Therefore, the WRF-CMAQ model using our configuration can generally reproduce the characteristics of O_3 and meteorological factors during the study period, and thereby can provide valuable insights into the formation of the O_3 pollution episode.

3. Results

3.1. Ozone Pollution Episode Affected by TC Jongdari

Similar to other cities in the Yangtze River Delta, Suzhou experiences more O_3 pollution episodes in June due to calm weather conditions associated with high-pressure systems, and O_3 pollution episodes in July or August often coincide with TCs (Zhan et al., 2020). In general, TCs generated over the western North Pacific follow three prevailing tracks: westward moving, northwestward moving or northeastward recurving. While TCs landing in the Yangtze River Delta mainly take a northwestward track (Wu et al., 2011), which can play a crucial role in the ecological environment. A typical example is that TC Jongdari caused the most serious O_3 pollution in Suzhou in the summer of 2018 on July 28 (Figure 1). Before TC Jongdari approached and brought rain, Suzhou was controlled by strong downdrafts induced by the periphery of TC (Figure 3a). Downdrafts could inhibit the development of convection, trap heat, and form a stable atmospheric structure (The average T_2 exceeded 31°C and the average WS_{10} was less than 1.5 m/s from July 27 to 30.). High temperature was beneficial to the photochemical O_3 production, while downdrafts and weak winds created a poor dispersion environment for O_3, which was the main reason for this O_3 pollution episode (Zhan and Xie, 2022b). However, from the perspective of O_3 transport, this O_3 pollution episode could be further divided into two phases.

3.1.1. July 27 to 28: Westward Transport of O_3 Driven by Sea Breeze

Under calm or weak wind conditions, Suzhou could experience both lake and sea breezes that had important impacts on O_3 pollution during the day. The westerly lake breeze was obvious around noon, and the easterly sea breeze intensified in the afternoon. The lake breeze only affected tens of kilometers around Lake Taihu. But the sea breeze combined with background southeasterly winds could extend its range up to 100–200 km inland from the shoreline (Figure S6 in Supporting Information S1). In vertical direction, both lake and sea breezes appeared below 1.5 km from the ground (Figure S7 in Supporting Information S1). In terms of intensity, the lake breeze typically remained below 2 m/s, whereas the sea breeze could occasionally exceed 4 m/s (Figure S8a in Supporting Information S1).

Since the lake and sea breezes were in opposite directions, O_3 pollution zone was usually found where they meet. And the location of the O_3 pollution zone was sensitive to the onset and end times, intensity and influence range of lake and sea breezes. On July 27, lake breeze was observed until late afternoon. The persistent westerly wind over the lake pushed O_3 pollution downstream to the east of Suzhou by about 30 km, and the MDA8 O_3 concentration in Suzhou that day did not exceed the national standard. In contrast, sea breeze developed well on the afternoon of July 28. The sea breeze passed through heavily polluted areas such as Shanghai and continued to erode the territory of the lake breeze, approaching Suzhou. As a consequence, Suzhou encountered severe O_3 pollution on that day, with the MDA8 O_3 concentration as high as 251 μg/m^3 (Figure S6 in Supporting Information S1).

3.1.2. July 28 to 29: Eastward Transport of O_3 Driven by Lake Breeze

O_3 had a strong diurnal variation, with the highest in the afternoon and the lowest in the early morning. The afternoon surface O_3 maximum was the result of strong photochemical reactions and good vertical mixing occurring in the boundary layer. The morning surface O_3 minimum, especially in urban areas, was due to NO titration ($O_3 + NO \rightarrow O_2 + NO_2$) and surface deposition. However, on water surfaces, NO titration was reduced because of low NO_x concentrations, and O_3 removal by deposition was also reduced as O_3 was poorly water-soluble. Therefore, lake became natural "pool" of O_3 through retaining air pollutants at night (Zeren et al., 2022). On the afternoon of July 28, sea breeze drove O_3 to be transported westward through Suzhou and then to Lake Taihu. A considerable portion of O_3 was retained in the residual layer above the lake, forming an O_3
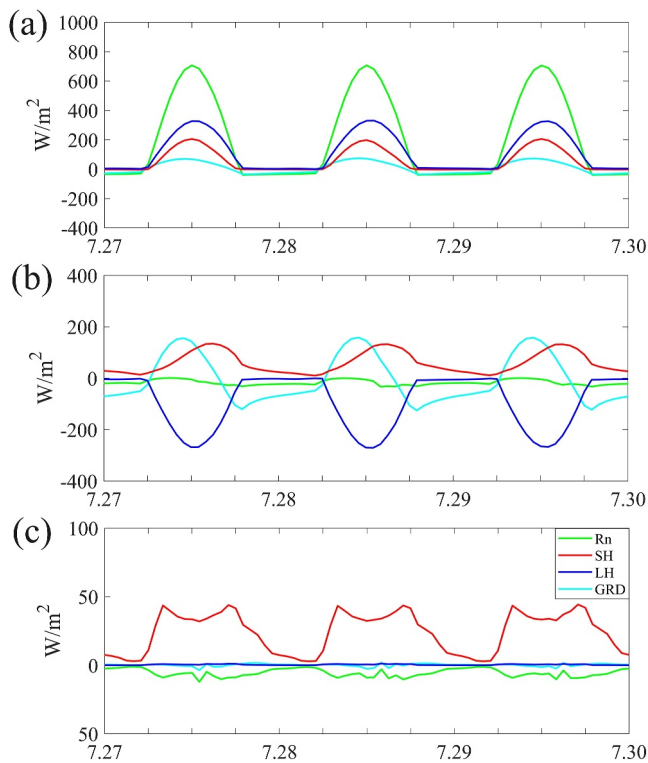
Figure 2. (a) Time series of net radiation (Rn, green lines), sensible heat flux (SH, red lines), latent heat flux (LH, blue lines) and ground heat flux (GRD, cyan lines) averaged over Suzhou urban areas in USGS-noAH simulation from July 27 to 30. The urban areas are based on GLC land use. (b) and (c) show the differences between GLC-noAH and USGS-noAH (GLC-noAH minus USGS-noAH), and GLC-AH and GLC-noAH (GLC-AH minus GLC-noAH).

"pool" at night. After sunrise, the nocturnal residual layer was destroyed and air mass with rich O_3 was transported downward and then moved eastward driven by the lake breeze, which played a vital role in the O_3 pollution in Suzhou on July 29 (Figure S7 in Supporting Information S1).

3.2. Surface Energy Balance Modified by Urbanization

Surface energy balance is a fundamental starting point for understanding changes induced by urbanization. It is the net radiation, which is the sum of shortwave radiation and longwave radiation, balanced by sensible, latent and ground heat fluxes (Oke et al., 2017). In the USGS-noAH simulation, most of Suzhou was covered by cropland. The surface soil was moist and evapotranspiration was active. The average latent heat flux in Suzhou was 113.3 W/m^2, almost twice the sensible heat flux (57.2 W/m^2). The surface energy balance was mainly dominated by net radiation and latent heat flux (Figure 2a). With the process of urbanization, cropland was gradually replaced by impervious surfaces in the GLC-noAH simulation. The effective moisture of the surface soil was low, leading to an increase in sensible heat flux of 59.6 W/m^2 and a decrease in latent heat flux of 92.5 W/m^2. Impervious surfaces had higher heat storage capacity and more heat transport to the deeper soil, thereby increasing ground heat flux. On the other hand, with more impervious surfaces, the albedo decreased from 0.187 to 0.168, resulting in more shortwave radiation during the day. However, this effect was overshadowed by more longwave radiation due to higher skin temperatures, and the net radiation ultimately dropped by 17.1 W/m^2. In this case, the net radiation in urban areas was partitioned into sensible heat flux and ground heat flux, rather than latent heat flux (Figure 2b). Almost all energy used for human purposes is eventually dissipated as heat. This excess heat, commonly referred to as AH, can be injected directly into the atmosphere. In the GLC-AH simulation, AH with its diurnal variation was added to the sensible heat item in WRF. The added heat flux increased the sensible heat flux by 24.1 W/m^2, accounting for 17.1% of the sensible heat flux. The skin temperature increased as well, leading to an increase in longwave radiation, followed by a slight decrease in net radiation of 5.5 W/m^2. As for the latent heat flux and ground heat flux, they remained almost the same when the AH flux was taken into account (Figure 2c).

Overall, urbanization fundamentally modified the surface energy balance. With more urban LU and AH, there was a decrease in net radiation and latent heat flux, and an increase in sensible and ground heat fluxes. Furthermore, the distribution of surface heat flux in urbanized area was mainly dominated by sensible heat flux.

3.3. Impacts of Urbanization-Modified Thermal Circulations on O_3

Due to higher sensible heat flux during the day and release of stored heat at night, urban areas are almost always warmer than their surroundings. This phenomenon is widely known as urban heat island (UHI) that can trigger urban heat island circulation (UHIC). In the USGS-noAH simulation, UHIC was identifiable despite small urban area of Suzhou in the late 1980s. This circulation was more evident at noon and extended vertically to about 2 km from the ground to the top of the urban boundary layer. It promoted the vertical mixing of O_3 in the boundary layer, which was an important way to maintain high concentration of O_3 at surface during the day (Figure 3a). Urbanization can enhance surface heating via increased sensible heat flux from more urban LU and AH (Section 3.2). In the GLC-noAH simulation, T_2 increased by 1.1°C when using the updated GLC LU data. The warming in the T_2 period could enhance the UHIC and promote the boundary layer height (PBLH) to increase by 96.2 m. The lake breeze near noon also increased by about 0.1 m/s due to the increase in urban-lake temperature difference. Nonetheless, the increase in temperature gradient was not significant since Suzhou is far from the coastline. In addition, urban expansion increased surface roughness, resulting in the easterly wind composed of sea breeze and background wind weakening by about 0.3 m/s when passing through Suzhou (Figure S8b in Supporting Information S1). Compared with LU, the changes induced by AH were much smaller. T_2 and PBLH
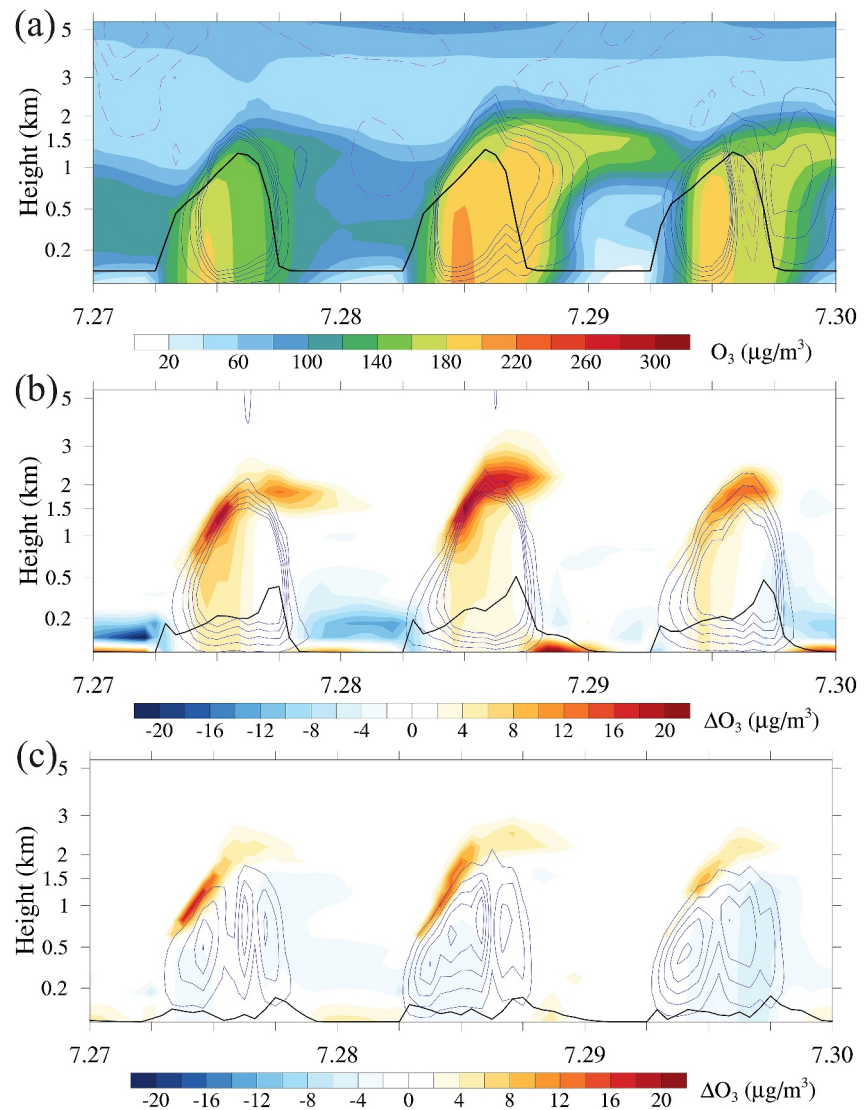
Figure 3. (a) Temporal-vertical distribution of O_3 (colored shading), boundary layer height (black line) and vertical wind velocity over Suzhou urban areas in USGS-noAH simulation from July 27 to 30. The urban areas are based on GLC land use. The dotted purple line and solid blue line indicate downward airflows and upward airflows. (b) and (c) show the differences between GLC-noAH and USGS-noAH (GLC-noAH minus USGS-noAH), and GLC-AH and GLC-noAH (GLC-AH minus GLC-noAH).

increased by 0.3°C and 27.0 m in the GLC-AH simulation. Regarding thermal circulations, the UHIC was enhanced. Except for UHIC, AH had little impact on lake or sea breezes, but AH could transfer momentum downward, complementing the wind reduction caused by urban surface friction. This was also confirmed by the larger WS_{10} in the GLC-AH simulation than in the GLC-noAH simulation (Figure S8c in Supporting Information S1).

Modification of boundary layer structure and thermal circulations further affected O_3 distribution, but the impact varied between day and night. Updating the LU from USGS to GLC resulted in an increase in temperature and enhanced UHIC. During the day, the increase in temperature was conducive to photochemical reactions, causing a rise of O_3 concentration throughout the boundary layer. Meanwhile, the enhanced upward motion generally transported O_3 from the middle to the upper boundary layer, culminating in an O_3 accumulation at the top of the boundary layer. At night, O_3 chemistry was controlled by NO titration. The transport of NO_x near the surface to the upper air through upward motion dominated the increase of surface O_3 and the decrease of O_3 aloft (Figure 3b). Similar to urban LU, AH also increased temperature and intensified upward motion, which in turn
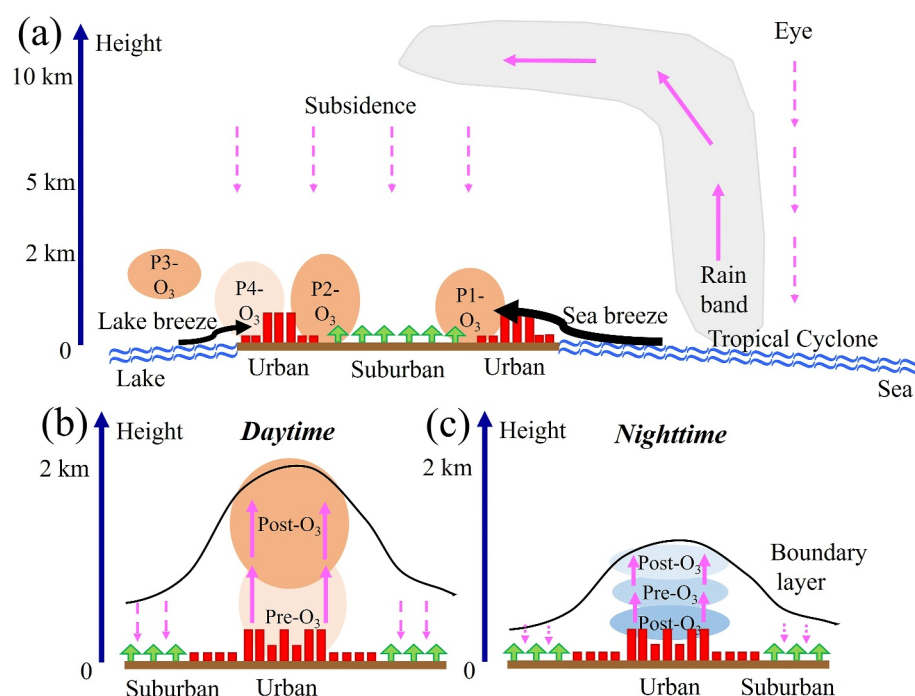
Figure 4. Schematic diagram showing how urbanization-modified thermal circulations alter O_3 transport affected by peripheral subsidence of TCs. The dotted and solid purple lines indicate downward and upward airflows. The red bars and green arrows represent urban and suburban areas. In (a), P1-O_3, P2-O_3, P3-O_3 and P4-O_3 refer to O_3 air masses at different phases driven by sea or lake breezes. In (b) and (c), Pre-O_3 and Post-O_3 refer to O_3 air masses before and after urbanization. The black line represents boundary layer height. Darker orange or blue represents air masses with higher O_3 concentration.

resulted in elevated O_3 in the upper boundary layer during the day and near the surface at night, albeit to a smaller magnitude (Figure 3c). Furthermore, the diurnal variation of AH exhibited a bimodal pattern (Figure 2c), and the spatial distribution of AH was uneven (Figure S3 in Supporting Information S1). These made AH-induced warming and upward motion more fragmented than urban LU, weakening the "collective effect" of the whole city. As a result, photochemical generation and vertical transport of O_3 were attenuated during the day (Figures S9 and S10 in Supporting Information S1).

4. Summary and Discussions

In this study, we report a prominent case observed in Suzhou, a megacity in eastern China, to explore the impact of urbanization-modified thermal circulations on O_3 transport during TCs. By combining in-situ observations and model results, it was found that under the control of peripheral subsidence of TC Jongdari, O_3 pollution and thermal circulations including sea and lake breezes were prone to appear. These thermal circulations had different onset and end times, which would lead to relay transport of O_3. As illustrated in Figure 4a, in the afternoon, the easterly sea breeze transported O_3-polluted air masses westward (P1-O_3), causing the first O_3 pollution when passing through Suzhou (P2-O_3). At night, a large amount of O_3 was stored over the lake (P3-O_3). On the second morning, the westerly lake breeze would transport O_3 back to Suzhou, contributing to the second O_3 pollution (P4-O_3). This relay transport of O_3 caused repeated O_3 pollution and thereby prolonged the duration of O_3 pollution. Urbanization altered the surface energy balance, enhancing surface heating and UHIC mainly through sensible heat flux increased by urban LU and AH. During the day, enhanced photochemical reactions generate more O_3, although some O_3 was transported to the upper boundary layer (Figure 4b). At night, NO_x was also transported upward, which on the contrary causes O_3 concentration increase at surface and decrease in the upper boundary layer due to NO titration (Figure 4c). In summary, urbanization would increase surface O_3 concentration regardless of day or night, making O_3 pollution worse. However, fragmented urban LU and AH emissions could weaken the collective effect of cities, thereby alleviating urban O_3 pollution to a certain extent.

This study highlights the importance of multiple thermal circulations interactions on O_3 transport. Moreover, things will be more complicated with urbanization. To improve urban air quality, research on this topic should be encouraged, especially for rapidly developing areas with diverse topography.

Data Availability Statement

Air pollutants monitoring data are available at https://quotsoft.net/air/, users can click on "China Air Quality Data" to download the data via Baidu Cloud. The best-track dataset provided by the CMA can be obtained from https://tcdata.typhoon.org.cn/en/zjljsjj.html ("Best Track Data", Lu et al., 2021). The NCEP FNL data are available at https://rda.ucar.edu/datasets/ds083.2/ (National Centers for Environmental Prediction/National Weather Service/NOAA/U.S. Department of Commerce, 2000). The MEIC data are accessible at http://meic-model.org.cn/?page_id=541&lang=en (Version 1.4, Zheng et al., 2018). These data can be downloaded for free as long as you agree to the official instructions. Meteorological data are also provided by the CMA. Due to the data policy in China, these data records are not available via a website for public download. But anyone can contact the China Meteorological Data Service Center for detailed information on data acquisition (http://data.cma.cn/en/?r=data/detail&dataCode=A.0012.0001).

References

Arnfield, A. J. (2003). Two decades of urban climate research: A review of turbulence, exchanges of energy and water, and the urban heat island. *International Journal of Climatology*, 23(1), 1–26. https://doi.org/10.1002/joc.859

Atkinson, R. (2000). Atmospheric chemistry of VOCs and NOx. *Atmospheric Environment*, 34(12–14), 2063–2101. https://doi.org/10.1016/S1352-2310(99)00460-4

Deng, T., Wang, T., Wang, S., Zou, Y., Yin, C., Li, F., et al. (2019). Impact of typhoon periphery on high ozone and high aerosol pollution in the Pearl River Delta region. *Science of the Total Environment*, 668, 617–630. https://doi.org/10.1016/j.scitotenv.2019.02.450

Flanner, M. G. (2009). Integrating anthropogenic heat flux with global climate models. *Geophysical Research Letters*, 36(2). https://doi.org/10.1029/2008gl036465

Goldberg, D. L., Vinciguerra, T. P., Hosley, K. M., Loughner, C. P., Canty, T. P., Salawitch, R. J., & Dickerson, R. R. (2015). Evidence for an increase in the ozone photochemical lifetime in the eastern United States using a regional air quality model. *Journal of Geophysical Research: Atmospheres*, 120(24), 12778–12793. https://doi.org/10.1002/2015jd023930

Gong, C., Liao, H., Zhang, L., Yue, X., Dang, R., & Yang, Y. (2020). Persistent ozone pollution episodes in North China exacerbated by regional transport. *Environmental Pollution*, 265, 115056. https://doi.org/10.1016/j.envpol.2020.115056

Gong, P., Liu, H., Zhang, M., Li, C., Wang, J., Huang, H., et al. (2019). Stable classification with limited sample: Transferring a 30-m resolution sample set collected in 2015 to mapping 10-m resolution global land cover in 2017. *Science Bulletin*, 64(6), 370–373. https://doi.org/10.1016/j.scib.2019.03.002

Iacono, M. J., Delamere, J. S., Mlawer, E. J., Shephard, M. W., Clough, S. A., & Collins, W. D. (2008). Radiative forcing by long-lived greenhouse gases: Calculations with the AER radiative transfer models. *Journal of Geophysical Research*, 113(D13). https://doi.org/10.1029/2008JD009944

Iannarelli, A. M., Di Bernardino, A., Casadio, S., Bassani, C., Cacciani, M., Campanelli, M., et al. (2022). The boundary layer air quality-analysis using network of instruments (BAQUNIN) supersite for atmospheric research and satellite validation over Rome area. *Bulletin of the American Meteorological Society*, 103(2), E599–E618. https://doi.org/10.1175/bams-d-21-0099.1

Janjić, Z. I. (1994). The step-mountain eta coordinate model: Further developments of the convection, viscous sublayer, and turbulence closure schemes. *Monthly Weather Review*, 122(5), 927–945. https://doi.org/10.1175/1520-0493(1994)122<0927:TSMECM>2.0.CO;2

Jiang, X., Wiedinmyer, C., Chen, F., Yang, Z. L., & Lo, J. C. F. (2008). Predicted impacts of climate and land use change on surface ozone in the Houston, Texas, area. *Journal of Geophysical Research*, 113(D20). https://doi.org/10.1029/2008jd009820

Jiang, Y. C., Zhao, T. L., Liu, J., Xu, X. D., Tan, C. H., Cheng, X. H., et al. (2015). Why does surface ozone peak before a typhoon landing in southeast China? *Atmospheric Chemistry and Physics*, 15(23), 13331–13338. https://doi.org/10.5194/acp-15-13331-2015

Kain, J. S. (2004). The kain–fritsch convective parameterization: An update. *Journal of Applied Meteorology*, 43(1), 170–181. https://doi.org/10.1175/1520-0450(2004)043<0170:TKCPAU>2.0.CO;2

Kang, H., Zhu, B., Gao, J., He, Y., Wang, H., Su, J., et al. (2019). Potential impacts of cold frontal passage on air quality over the Yangtze River Delta, China. *Atmospheric Chemistry and Physics*, 19(6), 3673–3685. https://doi.org/10.5194/acp-19-3673-2019

Lelieveld, J., Evans, J. S., Fnais, M., Giannadaki, D., & Pozzer, A. (2015). The contribution of outdoor air pollution sources to premature mortality on a global scale. *Nature*, 525(7569), 367–371. https://doi.org/10.1038/nature15371

Li, K., Jacob, D. J., Shen, L., Lu, X., De Smedt, I., & Liao, H. (2020). Increases in surface ozone pollution in China from 2013 to 2019: Anthropogenic and meteorological influences. *Atmospheric Chemistry and Physics*, 20(19), 11423–11433. https://doi.org/10.5194/acp-20-11423-2020

Li, M., Mao, Z., Song, Y., Liu, M., & Huang, X. (2015). Impacts of the decadal urbanization on thermally induced circulations in eastern China. *Journal of Applied Meteorology and Climatology*, 54(2), 259–282. https://doi.org/10.1175/jamc-d-14-0176.1

Li, M., Song, Y., Mao, Z., Liu, M., & Huang, X. (2016). Impacts of thermal circulations induced by urbanization on ozone formation in the Pearl River Delta region, China. *Atmospheric Environment*, 127, 382–392. https://doi.org/10.1016/j.atmosenv.2015.10.075

Liao, J., Wang, T., Jiang, Z., Zhuang, B., Xie, M., Yin, C., et al. (2015). WRF/Chem modeling of the impacts of urban expansion on regional climate and air pollutants in Yangtze River Delta, China. *Atmospheric Environment*, 106, 204–214. https://doi.org/10.1016/j.atmosenv.2015.01.059

Liu, Y., & Wang, T. (2020). Worsening urban ozone pollution in China from 2013 to 2017 – Part1: The complex and varying roles of meteorology. *Atmospheric Chemistry and Physics*, 20(11), 6305–6321. https://doi.org/10.5194/acp-20-6305-2020

Lu, X., Yu, H., Ying, M., Zhao, B., Zhang, S., Lin, L., et al. (2021). Western North pacific tropical cyclone database created by the China meteorological administration. *Advances in Atmospheric Sciences*, 38(4), 690–699. https://doi.org/10.1007/s00376-020-0211-7

Miao, Y., Guo, J., Liu, S., Liu, H., Zhang, G., Yan, Y., & He, J. (2017). Relay transport of aerosols to Beijing-Tianjin-Hebei region by multi-scale atmospheric circulations. *Atmospheric Environment*, *165*, 35–45. https://doi.org/10.1016/j.atmosenv.2017.06.032

Monks, P. S., Archibald, A. T., Colette, A., Cooper, O., Coyle, M., Derwent, R., et al. (2015). Tropospheric ozone and its precursors from the urban to the global scale from air quality to short-lived climate forcer. *Atmospheric Chemistry and Physics*, *15*(15), 8889–8973. https://doi.org/10.5194/acp-15-8889-2015

National Centers for Environmental Prediction/National Weather Service/NOAA/U.S. Department of Commerce. (2000). NCEP FNL operational model global tropospheric Analyses, continuing from july 1999. (Updated daily) [Dataset]. https://doi.org/10.5065/D6M043C6. *Research Data Archive at the National Center for Atmospheric Research, Computational and Information Systems Laboratory*.

Oke, T. R., Mills, G., & Voogt, J. A. (2017). *Urban climates* (pp. 77–121). Cambridge University Press.

Ribeiro, F. N. D., Oliveira, A. P. d., Soares, J., Miranda, R. M. d., Barlage, M., & Chen, F. (2018). Effect of sea breeze propagation on the urban boundary layer of the metropolitan region of Sao Paulo, Brazil. *Atmospheric Research*, *214*, 174–188. https://doi.org/10.1016/j.atmosres.2018.07.015

Ryu, Y. H., Baik, J. J., Kwak, K. H., Kim, S., & Moon, N. (2013). Impacts of urban land-surface forcing on ozone air quality in the Seoul metropolitan area. *Atmospheric Chemistry and Physics*, *13*(4), 2177–2194. https://doi.org/10.5194/acp-13-2177-2013

Sullivan, J. T., McGee, T. J., Langford, A. O., Alvarez, R. J., Senff, C. J., Reddy, P. J., et al. (2016). Quantifying the contribution of thermally driven recirculation to a high-ozone event along the Colorado Front Range using lidar. *Journal of Geophysical Research: Atmospheres*, *121*(17), 10377–310390. https://doi.org/10.1002/2016jd025229

Tewari, M., Chen, F., Wang, W., Dudhia, J., LeMone, M. A., Mitchell, K., et al. (2004). Implementation and verification of the unified NOAH land surface model in the WRF model. *20th Conference on Weather Analysis and Forecasting/16th Conference on Numerical Weather Prediction*, 11–15.

Thompson, G., Field, P. R., Rasmussen, R. M., & Hall, W. D. (2008). Explicit forecasts of winter precipitation using an improved bulk microphysics scheme. Part II: Implementation of a new snow parameterization. *Monthly Weather Review*, *136*(12), 5095–5115. https://doi.org/10.1175/2008MWR2387.1

Tian, M., Wang, H., Chen, Y., Yang, F., Zhang, X., Zou, Q., et al. (2016). Characteristics of aerosol pollution during heavy haze events in Suzhou, China. *Atmospheric Chemistry and Physics*, *16*(11), 7357–7371. https://doi.org/10.5194/acp-16-7357-2016

Wang, T., Xue, L., Brimblecombe, P., Lam, Y. F., Li, L., & Zhang, L. (2017). Ozone pollution in China: A review of concentrations, meteorological influences, chemical precursors, and effects. *Science of the Total Environment*, *575*, 1582–1596. https://doi.org/10.1016/j.scitotenv.2016.10.081

Wang, T., Xue, L., Feng, Z., Dai, J., Zhang, Y., & Tan, Y. (2022). Ground-level ozone pollution in China: A synthesis of recent findings on influencing factors and impacts. *Environmental Research Letters*, *17*(6), 063003. https://doi.org/10.1088/1748-9326/ac69fe

Wang, W., Parrish, D. D., Wang, S., Bao, F., Ni, R., Li, X., et al. (2022). Long-term trend of ozone pollution in China during 2014–2020: Distinct seasonal and spatial characteristics and ozone sensitivity. *Atmospheric Chemistry and Physics*, *22*(13), 8935–8949. https://doi.org/10.5194/acp-22-8935-2022

Wei, J., Li, Z., Li, K., Dickerson, R. R., Pinker, R. T., Wang, J., et al. (2022). Full-coverage mapping and spatiotemporal variations of ground-level ozone (O_3) pollution from 2013 to 2020 across China. *Remote Sensing of Environment*, *270*, 112775. https://doi.org/10.1016/j.rse.2021.112775

Wu, L., Zong, H., & Liang, J. (2011). Observational analysis of sudden tropical cyclone track changes in the vicinity of the east China sea. *Journal of the Atmospheric Sciences*, *68*(12), 3012–3031. https://doi.org/10.1175/2010JAS3559.1

Xie, M., Liao, J., Wang, T., Zhu, K., Zhuang, B., Han, Y., et al. (2016a). Modeling of the anthropogenic heat flux and its effect on regional meteorology and air quality over the Yangtze River Delta region, China. *Atmospheric Chemistry and Physics*, *16*(10), 6071–6089. https://doi.org/10.5194/acp-16-6071-2016

Xie, M., Zhu, K., Wang, T., Feng, W., Gao, D., Li, M., et al. (2016b). Changes in regional meteorology induced by anthropogenic heat and their impacts on air quality in South China. *Atmospheric Chemistry and Physics*, *16*(23), 15011–15031. https://doi.org/10.5194/acp-16-15011-2016

Xue, L. K., Wang, T., Gao, J., Ding, A. J., Zhou, X. H., Blake, D. R., et al. (2014). Ground-level ozone in four Chinese cities: Precursors, regional transport and heterogeneous processes. *Atmospheric Chemistry and Physics*, *14*(23), 13175–13188. https://doi.org/10.5194/acp-14-13175-2014

You, C., Chi-Hung Fung, J., & Tse, W. P. (2019). Response of the sea breeze to urbanization in the pearl River Delta region. *Journal of Applied Meteorology and Climatology*, *58*(7), 1449–1463. https://doi.org/10.1175/jamc-d-18-0081.1

Young, P. J., Archibald, A. T., Bowman, K. W., Lamarque, J. F., Naik, V., Stevenson, D. S., et al. (2013). Pre-industrial to end 21st century projections of tropospheric ozone from the atmospheric chemistry and climate model intercomparison project (ACCMIP). *Atmospheric Chemistry and Physics*, *13*(4), 2063–2090. https://doi.org/10.5194/acp-13-2063-2013

Zeren, Y., Zhou, B., Zheng, Y., Jiang, F., Lyu, X., Xue, L., et al. (2022). Does ozone pollution share the same formation mechanisms in the bay areas of China? *Environmental Science & Technology*, *56*(20), 14326–14337. https://doi.org/10.1021/acs.est.2c05126

Zhan, C., & Xie, M. (2022a). Land use and anthropogenic heat modulate ozone by meteorology: A perspective from the Yangtze River Delta region. *Atmospheric Chemistry and Physics*, *22*(2), 1351–1371. https://doi.org/10.5194/acp-22-1351-2022

Zhan, C., & Xie, M. (2022b). Exploring the link between ozone pollution and stratospheric intrusion under the influence of tropical cyclone Ampil. *Science of the Total Environment*, *828*, 154261. https://doi.org/10.1016/j.scitotenv.2022.154261

Zhan, C., Xie, M., Huang, C., Liu, J., Wang, T., Xu, M., et al. (2020). Ozone affected by a succession of four landfall typhoons in the Yangtze River Delta, China: Major processes and health impacts. *Atmospheric Chemistry and Physics*, *20*(22), 13781–13799. https://doi.org/10.5194/acp-20-13781-2020

Zhan, C., Xie, M., Liu, J., Wang, T., Xu, M., Chen, B., et al. (2021). Surface ozone in the Yangtze River Delta, China: A synthesis of basic features, meteorological driving factors, and health impacts. *Journal of Geophysical Research: Atmospheres*, *126*(6). https://doi.org/10.1029/2020jd033600

Zhang, N., Zhu, L., & Zhu, Y. (2011). Urban heat island and boundary layer structures under hot weather synoptic conditions: A case study of Suzhou city, China. *Advances in Atmospheric Sciences*, *28*(4), 855–865. https://doi.org/10.1007/s00376-010-0040-1

Zhang, Q., Zheng, Y., Tong, D., Shao, M., Wang, S., Zhang, Y., et al. (2019). Drivers of improved $PM_{2.5}$ air quality in China from 2013 to 2017. *Proceedings of the National Academy of Sciences*, *116*(49), 24463–24469. https://doi.org/10.1073/pnas.1907956116

Zhang, X., Ma, Q., Chu, W., Ning, M., Liu, X., Xiao, F., et al. (2023). Identify the key emission sources for mitigating ozone pollution: A case study of urban area in the Yangtze River Delta region, China. *Science of the Total Environment*, *892*, 164703. https://doi.org/10.1016/j.scitotenv.2023.164703

Zhang, Y., Yang, P., Gao, Y., Leung, R. L., & Bell, M. L. (2020). Health and economic impacts of air pollution induced by weather extremes over the continental US. *Environment International*, *143*, 105921. https://doi.org/10.1016/j.envint.2020.105921

Zhao, H., Chen, K., Liu, Z., Zhang, Y., Shao, T., & Zhang, H. (2021). Coordinated control of $PM_{2.5}$ and O_3 is urgently needed in China after implementation of the "Air pollution prevention and control action plan. *Chemosphere*, *270*, 129441. https://doi.org/10.1016/j.chemosphere.2020.129441

Zheng, B., Tong, D., Li, M., Liu, F., Hong, C., Geng, G., et al. (2018). Trends in China's anthropogenic emissions since 2010 as the consequence of clean air actions. *Atmospheric Chemistry and Physics*, *18*(19), 14095–14111. https://doi.org/10.5194/acp-18-14095-2018

References From the Supporting Information

Huang, C., Wang, T., Niu, T., Han, J., Li, M., Zhang, N., et al. (2021). Study on the causes of heavy pollution in Shenyang based on the contribution of natural conditions, physical processes, and anthropogenic emissions. *Atmospheric Pollution Research*, *12*(11), 101224. https://doi.org/10.1016/j.apr.2021.101224

Li, M., Wang, T., Xie, M., Zhuang, B., Li, S., Han, Y., et al. (2017). Improved meteorology and ozone air quality simulations using MODIS land surface parameters in the Yangtze River Delta urban cluster, China. *Journal of Geophysical Research: Atmospheres*, *122*(5), 3116–3140. https://doi.org/10.1002/2016jd026182

Zhu, J., Wang, T., Bieser, J., & Matthias, V. (2015). Source attribution and process analysis for atmospheric mercury in eastern China simulated by CMAQ-Hg. *Atmospheric Chemistry and Physics*, *15*(15), 8767–8779. https://doi.org/10.5194/acp-15-8767-2015